

# Dynamical Mean Field Theory of Temperature and Field Dependent Band Shifts in Magnetically Coupled Semimetals: Application to $EuB_6$

Chungwei Lin and Andrew J. Millis  
*Department of Physics, Columbia University*  
 538W 120th St NY, NY 10027

A model for semimetals such as  $EuB_6$ , in which band overlaps are controlled by magnetic order, is presented and is solved in the dynamical mean field approximation. First order phase boundaries are computed by evaluating free energies of different states. The phase diagram is determined. A specific and physically reasonable choice of parameters is found to approximately reproduce the available data on  $EuB_6$ . For this material, predictions are made for the location of a metamagnetic transition and its associated endpoint, and a change in the order of the magnetic transition.

PACS numbers: 71.10.+w, 71.27.+a, 75.10.-b, 78.20-e

## I. INTRODUCTION

$EuB_6$  is a magnetic semiconductor in which magnetic order apparently controls the bandgap. The ferromagnetic transition at  $T_c \sim 12K$  is signaled by a sharp increase in plasma frequency[1] and a sharp drop in resistivity[2] [3] [4]. In this paper we formulate a model which captures the physics of  $EuB_6$ , and solve it in the dynamical mean field approximation. The important technical step is the accurate determination of first order phase boundaries via the construction of the free energies of competing phases. We present a general phase diagram, which includes a change in the order of the transition from first to second. Remarkably, the change occurs not by the vanishing of a fourth order coefficient but simply by an exchange of stabilities. We show that for a choice of parameters consistent with what is calculated for  $EuB_6$  [6], the various experimental data are semiquantitatively reproduced. For these parameters, we predict that  $EuB_6$  should exhibit a metamagnetic phase transition, and we estimate the location of the transition line and its endpoints. The change in order of the phase transition might be accessible in pressure experiments. The analysis reported here may be thought of as a more precise solution of a model proposed by [6]. Our solution agrees with theirs in essential aspects but provides a sharper picture of physics and includes some new features.

We also note that the band structure of the material is presently the subject of controversy with photoemission experiments [7] indicating a large gap (implying that the material is intrinsically insulating so the metallic behavior is due to defects which dope the system) while some band calculations [5] [6] and quantum oscillation measurements[8] indicating a small negative gap causing the semimetal behavior. We comment below on the implications of our work for these controversies.

## II. MODEL HAMILTONIAN

The electronic structure of  $EuB_6$  has been calculated [5] [6]. Experiment, quantum chemical intuition and band calculations all agree that the  $Eu f$ -shell is half filled and, as the scale relevant for electronic behavior, electronically inert. Crystal field effects are negligible and to a good approximation, each  $Eu$  may be regarded as carrying a  $S = 7/2$  "core spin". Band theory calculations [6] reveal two near Fermi surface bands: a nearly empty band with a minimum at X-point, derived mainly from  $Eu-d$ ,  $B-p$  orbitals, and a nearly full band with a maximum at the X-point, derived mainly from  $Eu-f$ ,  $B-p$  ones. The hybridization between these bands is negligible because they arise from different symmetry orbitals.

Because we shall be interested in low energies and weak couplings, we expand the bands near the X-point so the minimal model describing  $EuB_6$  becomes:

$$\begin{aligned}
 H = & \sum_{\sigma, \vec{p}} \left( \frac{p^2}{2m_1} + \Delta \right) c_{1, \sigma, \vec{p}}^+ c_{1, \sigma, \vec{p}} - \frac{p^2}{2m_2} c_{2, \sigma, \vec{p}}^+ c_{2, \sigma, \vec{p}} \\
 & + \sum_{i, a, b, \alpha, \beta} J^{a, b} \vec{S}_i \cdot c_{a, i, \alpha}^+ \vec{\sigma}_{\alpha \beta} c_{b, i, \beta} \\
 & - \mu \sum_i (n_{i, 1} + n_{i, 2})
 \end{aligned} \tag{1}$$

Here  $\vec{S}$  represents the  $S = 7/2$   $Eu$  core spin,  $c_1$  and  $c_2$  represent upper (conduction) and lower (valence) bands and  $\Delta$  controls the band overlap. We take  $|\vec{S}| = 1$ , absorbing the actual magnitude into the coupling  $J$ . Because  $\vec{S}$  originates from a filled (spin polarized)  $Eu$  shell, and the latest band structure calculation [6] shows that two bands arises from different  $Eu$  orbitals ( $f$  and  $d$ ), we may therefore take  $J$  to be diagonal in orbital indices. The high spin and low carrier density means the Kondo effect is irrelevant, so the sign of  $J$  is arbitrary. Kunes and Pickett's calculation [6] implies  $J^{11} < 0$  (Kondo coupling) and  $J^{22} > 0$  (anti-Kondo coupling) and indicates that the splitting of the conduction and valence bands are roughly the same, we choose  $J = J^{22} = -J^{11}$ . Our

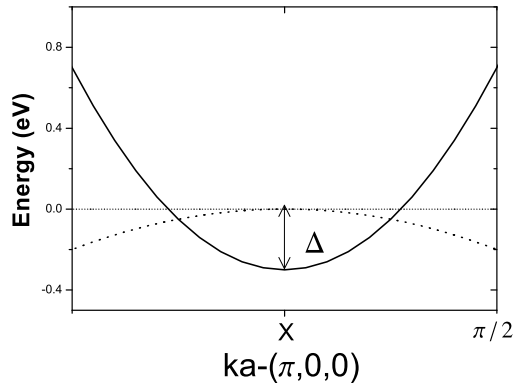


FIG. 1: Expanded view of ferromagnetic phase band structure of  $EuB_6$  with momentum  $k$  measured from  $X$   $[\pi, 0, 0]$ , in units of inverse lattice constant  $a = 4.2\text{\AA}$ . Curved (flat) dashed line represents valence (defect) band and heavy line conduction band.

results turn out to depend mainly on  $|J^{22}| + |J^{11}|$ . The chemical potential  $\mu$  is determined by the neutrality of the system, i.e. number of particles equals number of holes. Fig(1) shows the simplified band structure implied by eqn(1).

The model described in eqn(1) can be easily modified to match the bandstructure implied by the photoemission experiment[7] as follows: we interpret the lower band ( $c_2$ ) as arising from defect states which in this picture must exist so that carriers are donated to the conduction band, and thus take  $m_2$  to be infinite, and assure there is no coupling between  $c_2$  band and the core spin  $\vec{S}$  ( $J^{22} = 0$ ). At these parameters ( $m_2 \rightarrow \infty$ ,  $J^{22} = 0$ ), the  $c_2$  band serves as a particle reservoir and the chemical potential is fixed at 0. This choice in fact does not change the structure of the phase diagram or the qualitative features of our results.

The  $T = 0$  phase diagram is straightforward. The ground state is ferromagnetic. If  $\Delta + |J^{11}| + |J^{22}| < 0$ , the majority spin of band 1 crosses the minority spin of band 2, which results in metallic behavior. If not, the ground state is insulating. At  $T > T_c$ , the random spin orientations mean that the band shift are much less (especially at small  $J$ ). Roughly,  $\Delta < 0$  implies metallic behavior while  $\Delta > 0$  implies insulating state.

### III. BASIC RESULTS

#### A. Dynamical Mean Field and Free Energy

To study eqn(1), we use the single site dynamical mean field method [9]. This amounts to assuming that the electron self energy is momentum independent:  $\Sigma_{1,\sigma}(\vec{p}, \omega) \rightarrow \Sigma_{1,\sigma}(\omega)$ . The self energy is determined from the so-

lution of an auxiliary impurity model with free energy  $\Omega_{imp} = -T \log Z_{imp}$ , and

$$Z_{imp} = \int D[c^+ c] D[\vec{S}_c] \exp S_{eff}$$

with [11]

$$S_{eff} = \frac{1}{\beta^2} \int_0^\beta d\tau d\tau' \bar{c}_\alpha(\tau) a_{\alpha\beta}(\tau - \tau') c_\beta(\tau') + \frac{1}{\beta} \int d\tau J \vec{S} \cdot [\bar{\sigma}^{\alpha\beta} \bar{c}_\alpha(\tau) c_\beta(\tau) + h \hat{z}] \quad (2)$$

The free energy of the lattice model is [9]

$$\frac{\Omega}{N} = \Omega_{imp} - T \sum_{n,\sigma} \log G_\sigma(i\omega_n) - T \sum_{n,\sigma} \int d\epsilon D(\epsilon) \times \log[i\omega_n + \mu - \Sigma_\sigma(i\omega_n) - \epsilon] \quad (3)$$

and the auxiliary function  $a$  is fixed by the requirement  $\frac{\partial \Omega}{\partial a} = 0$ . It is important to perform the exact quantum trace over the spin degrees of freedom rather than employing the classical spin approximation often made [10] in order to obtain physically reasonable estimates for the entropy.

The free energy so determined is a functional of the applied field  $h$  and the system magnetization is given by  $m = -\frac{\partial \Omega}{\partial h}$ . It is sometimes useful to perform a Legendre transformation to obtain  $\Omega(m, T)$ . We have not found an efficient method for performing this transformation: to obtain  $\Omega(m, T)$ , we solve the dynamical mean field equations numerically for a range of  $h$ , and then construct  $\Omega(m, T) = \Omega(h, T) + h m$  explicitly. We note however that in some parameter ranges, the DMFT equations have two stable (symmetry un-related) solutions at  $h = 0$ , corresponding to states with  $m = 0$  and  $m \neq 0$ . The two states so determined are extrema of  $\Omega(m, T)$  and their free energies are the extremal values of  $\Omega(m, T)$ , so first order transition points may be located without constructing  $\Omega(m, T)$  explicitly.

#### B. Approximations and DMFT Solutions

We have solved the dynamical mean field equations corresponding to extremizing eqn(3) with respect to  $\Sigma(\omega_n)$ . For simplicity we adopted a semicircular density of states  $D(\epsilon) = \frac{\sqrt{4t^2 - \epsilon^2}}{2\pi t^2}$  with  $t = \frac{(\sqrt{2}\pi)^{\frac{1}{3}}}{ma^2}$  chosen to match the band theory band-edge density of states. We also assumed  $J/t \ll 1$  (because this is the limit relevant for the materials of interest) and  $T/J \ll 1$  (we will see below that the calculated transition temperature is much less than  $J$ ). These approximations simplify calculations considerably, in particular, in this limit we may retain only the  $z$  component of the core spin, simplifying the quantum trace.

To simplify the expression, we define

$$\Delta = 2yJ \quad (4)$$

where  $y$  is a dimensionless parameter measuring the bandgap. We also define the following  $f$  functions:

$$\begin{aligned} f^{15}(x) &= \Theta(x)x^{1.5} \\ f^{25}(x) &= \Theta(x)x^{2.5} \end{aligned}$$

where  $\Theta(x)$  is the step function.

In the small  $J$  limit,

$$\Sigma_{\uparrow,(\downarrow)} = \mp mJ \quad (5)$$

the free energy  $\Delta\Omega$  and core spin magnetization  $m$  are given by

$$\begin{aligned} \Delta\Omega(m) &= -\frac{4J}{15\pi} \times \\ &\left[ \left(\frac{J}{t_1}\right)^{3/2} (f^{25}(\mu - (y - m)) + f^{25}(\mu - (m + y))) \right. \\ &\left. + \left(\frac{J}{t_2}\right)^{3/2} (f^{25}(m - y - \mu) + f^{25}(-(m + y) - \mu)) \right] \\ &+ Tm\alpha - T \log \left[ \frac{\sinh[(1 + \frac{1}{2S})\alpha]}{\sinh[\frac{\alpha}{2S}]} \right] \end{aligned} \quad (6)$$

$$m = \frac{8}{7} \sinh\left(\frac{8\alpha}{7}\right) - \frac{1}{7} \sinh\left(\frac{\alpha}{7}\right) = B_{7/2}[\alpha(m, \beta)] \quad (7)$$

where

$$\begin{aligned} \alpha &= \frac{2}{3\pi} \beta J \times \\ &\left[ \left(\frac{J}{t_1}\right)^{1.5} (f^{15}(\mu - (y - m)) - f^{15}(\mu - (m + y))) + \right. \\ &\left. \left(\frac{J}{t_2}\right)^{1.5} (f^{15}(m - y - \mu) - f^{15}(-(m + y) - \mu)) \right] \end{aligned} \quad (8)$$

The chemical potential  $\mu$  is determined by charge neutrality, i.e. number of electron equals number of holes.

$$\begin{aligned} &\frac{1}{t_1^{1.5}} (f^{15}(\mu - (m - y)) + f^{15}(\mu - (m + y))) \\ &= \frac{1}{t_2^{1.5}} (f^{15}(m - y - \mu) + f^{15}(-(m + y) - \mu)) \end{aligned} \quad (9)$$

Note that  $\mu$  is a function of  $m$  and  $y$ , not an independent variable.

Based on the above expressions, the entropy  $S$  is

$$S = -\frac{\partial \Delta\Omega}{\partial T} = \log \left[ \frac{\sinh(\frac{8\alpha}{7})}{\sinh(\frac{\alpha}{7})} \right] - m\alpha \quad (10)$$

the specific heat  $C_V$  is

$$C_V = \frac{\partial \Delta E}{\partial T} = \frac{\partial(\Delta\Omega + TS)}{\partial T} = -T\alpha \frac{\partial m}{\partial T} \quad (11)$$

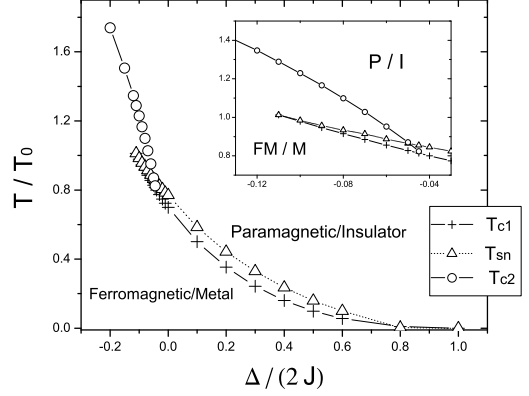


FIG. 2: The phase diagram. In the range  $-0.1J < \Delta < -0.55J$ , the system undergoes both 1st and 2nd order phase transitions. The temperature is in unit  $\frac{2}{3\pi} t_1 (\frac{J}{t_1})^{2.5}$ .  $T_0 = 17.43 K$  if the  $J = 0.16eV$  and  $t_1 = 1.16eV$  implied in Kunes/Pickett's bandstructure calculation.

$\frac{\partial m}{\partial T}$  can be computed from eqn(7).

Finally, the density of conducting band electrons  $\Delta n$  is

$$\begin{aligned} \Delta n &= \frac{4}{3\pi} \left(\frac{J}{t_1}\right)^{3/2} (f^{15}(\mu(m, y) - (y - m)) + \\ &f^{15}(\mu(m, y) - (m + y)) - 2 f^{15}(\mu(0, y) - y)) \end{aligned} \quad (12)$$

The plasma frequency  $\omega_p$  is defined as  $\omega_p^2 = 4\pi e^2 \frac{n}{m^*}$  and calculated by

$$\omega_p^2(T_c^-) - \omega_p^2(T_c^+) = 4\pi e^2 \frac{\Delta n}{2} \left( \frac{1}{m_1^*} + \frac{1}{m_2^*} \right) \quad (13)$$

We emphasize that all expressions above should be evaluated at the  $m$  where eqn(7) is satisfied.

The calculated phase diagram is shown in Fig(2). We see, in accord with the simple considerations of the previous section that for  $\Delta/J > 1$ , the material is always insulating and  $T_c$  is negligible. For  $\Delta$  sufficiently negative, the transition becomes second order.

Fig(3) shows the the free energy as a function of  $m$  at several temperatures and at different bandgaps. Panel (a) shows  $\Omega(m)$  for several  $T$  at  $\Delta/J = 0$ , in the first order region of the phase diagram. Panel b shows the unusual behavior in the vicinity of the multicritical point where the transition becomes second order. One naively expects the minimum at higher  $m$  shifts downwards, eventually merging with  $m = 0$  minimum (in other word, that the sign of the  $m^4$  term in the Landau expansion of the free energy changes). Panel (b) shows that the actual situation is more subtle: the higher  $m$  minimum continues to exist; however its energy is increased so the second order phase transition happens, and then at a lower temperature the higher minimum takes over. The temperature dependence of the magnetization in this region is

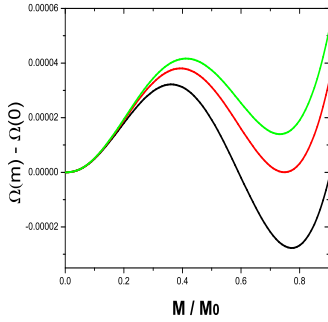
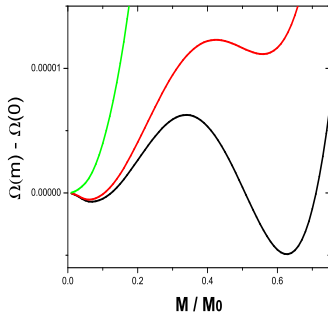
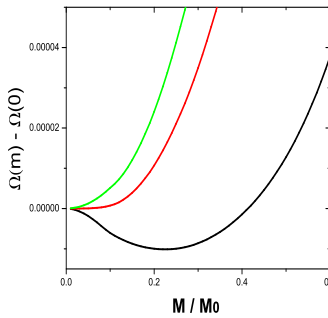
(a)  $\Delta = 0$ (b)  $\Delta = -0.14J$ (c)  $\Delta = -0.3J$ 

FIG. 3: Free Energy as a function of  $m$  at different temperature. (a)  $\Delta = 0$  where only first order phase transition occurs. From top to bottom:  $T > T_{c1}$ ,  $T = T_{c1}$ , and  $T < T_{c1}$ . (b)  $\Delta = -0.14J$  where both first and second phase transition occur. From top to bottom:  $T = T_{c2}$ ,  $T_{c2} > T > T_{c1}$ , and  $T < T_{c1}$ . (c)  $\Delta = -0.3J$  here only second order phase transition occurs. From top to bottom:  $T > T_{c2}$ ,  $T = T_{c2}$ , and  $T < T_{c2}$ .

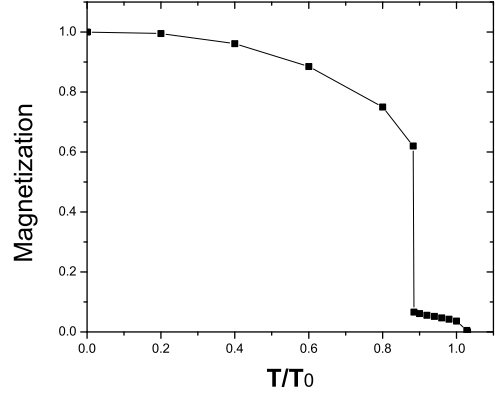


FIG. 4: The magnetization  $m$  in units of the  $T = 0$  saturation magnetization  $m_0$  as a function of temperature at  $\Delta = -0.14J$ .  $T_0 = 17.43 K$ . The second order transition at  $T \approx 1.028 T_0$ , followed by the first order transition at  $T \approx 0.89 T_0$ .

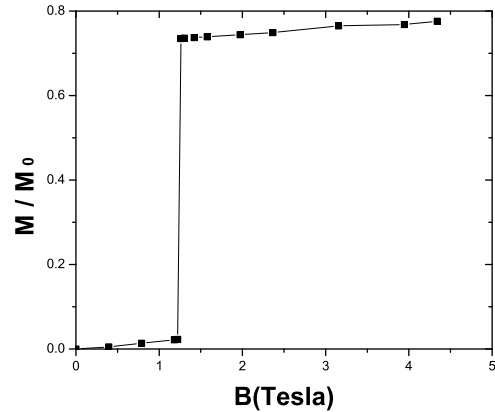


FIG. 5: The magnetization  $m$  in units of the  $T = 0$  saturation magnetization  $m_0$  in the paramagnetic phase at  $T = 12.55 K$  ( $T_c = 12.2 K$ ), as a function of magnetic field  $B$ , calculated from minimization of free energy for parameters  $t_1 = 1.16 eV$ ,  $t_2 = 0.68 eV$ ,  $J = 0.16 eV$ , appropriate to  $EuB_6$ .

shown in Fig(4). Finally, panel (c) shows the free energy in the region in which there is no first order transition at all. We note that pressure, by increasing hybridization, is expected to broaden bands, thereby makes  $\Delta$  more negative. The predicted change in order of transition may therefore be accessible in pressure experiments.

The presence, in the wide regions of the phase diagram, of a metastable high  $m$  free energy minimum, suggests that the system may undergo a metamagnetic phase transition. As shown in Fig(5), this is indeed the case.

#### IV. APPLICATION TO $EuB_6$

In this section, the model is applied to  $EuB_6$ . The literature presents two conflicting interpretations of this compound: the semimetal interpretation favored by quantum oscillations[8] and bandstructure calculations[6], and the large band gap interpretation, implied by photoemission[7]. These imply quite different parameters; we consider them separately, beginning with the semimetal case.

There are four parameters in this model – conduction and valence bandwidths  $t_1$  and  $t_2$ , coupling strength  $J$ , and the bandgap  $\Delta$ .  $t_1$  and  $t_2$  are fixed by the effective masses of both bands given in [6], and we found  $t_1 = 1.16 eV$ ,  $t_2 = 0.68 eV$ . Two sets of  $J$  and  $\Delta$  are chosen –  $J = 0.14 eV$ ,  $\Delta = -0.2J$  and  $J = 0.16 eV$ ,  $-0.04J < \Delta < 0.04J$ . The former choice are the best-fit parameters for fixed critical temperature and plasma frequency jump. However, these parameters produce a specific heat in disagreement with experiment and are in the region where the system has both 1st and 2nd order transitions whereas experiment apparently yields only one transition [3] We cannot fit  $T_c$  and  $\Delta\omega_p^2$  simultaneously in the 1st order transition region.  $J = 0.16 eV$ ,  $-0.04J < \Delta < 0.04J$  are chosen to match the critical temperature, but the calculated  $\Delta\omega_p^2$  and  $\Delta C_V$  are roughly 2.5 and 2 times larger than the experimental data.

With the two sets of parameters, we compute critical temperature  $T_c$ , jump in plasma frequency  $\Delta\omega_p^2$ , jump in specific heat  $\Delta C_V$ , core spin magnetization  $m$ , and latent heat  $\Delta Q$ . The results are summarized and compared with experiment in the following table.

Quantity	Expt	(0.14,-0.2J)	(0.16, ±0.04J)
$T_c$ (K)	12~14	12.2	12.2 ± 1
$\Delta\omega_p^2$ ( $10^7 cm^{-2}$ )	1.625	1.7	4.3 ± 0.2
$\Delta C_V$ (J/K per mole)	12	69.63 (10.47→80.1)	21.2 ± 2.4
$m / m_0$	*	0.3 (0.28→0.58)	0.75 ± 0.5
$\Delta Q$ (J/Mole)	*	30.92	90.5 ± 2

where the parentheses in the table represents  $(J(eV), \Delta)$ . For the parameters  $J = 0.14 eV$  and  $\Delta = -0.2J$ ,  $T_{c2} = 16.1 K$ .

The existence of a metastable  $m \neq 0$  state implies the existence of a metamagnetic phase transition. For example, Fig(5) shows  $M(B)$  calculated at a  $T$  slightly greater than  $T_c$ . We take  $T = 12.55K$  ( $T_c = 12.2K$ ). We see that the jump occurs at  $B = 1.12$  tesla, the magnetic field where the magnetization jump occurs as  $h^*$ , Fig(6) plots  $h^*$  as a function of temperature.

Photoemission experiments[7] at  $T > T_c$  detects a wide range band gap ( $\Delta \sim 1eV$ ), and a fermi level about  $0.2eV$  above the conduction band minimum. The carriers in this band must arise from defects which dope the system; we model the defects as a flat band ( $m_2 \rightarrow \infty$ ,

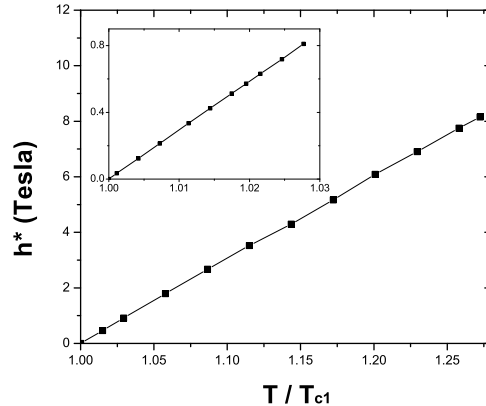


FIG. 6:  $h^*(T)$ , see the text for the definition of  $h^*$ . The metamagnetic phase transition ends at  $T = 1.28 T_{c1}$  for  $J = 0.16eV$ ,  $\Delta = 0$ . The inset is for parameters  $J = 0.2eV$ ,  $\Delta = -0.2J$  where the metamagnetic transition ends at  $T = 1.01T_{c1}$ .

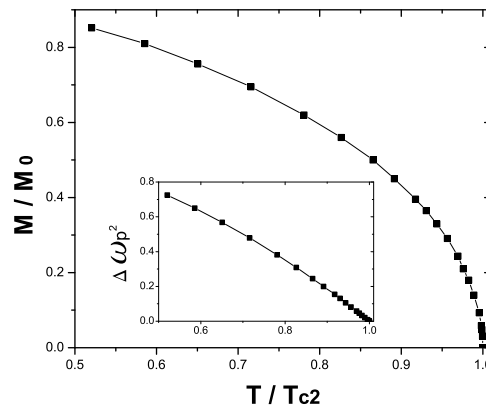


FIG. 7:  $M(T)$  at photoemission parameters.  $T_{c2} = 12.5K$ . The inset shows the square of plasma frequency ( $\Delta\omega_p^2$ ) (in the unit  $10^7 cm^{-2}$ ) as a function of temperature.

$t_2 = 0$ ). The measured conduction band dispersion implies  $t_1 = 1.54eV$ ; the fermi level position yields  $\Delta = -0.2eV$ ;  $J^2 = 0$ , and by fitting  $T_c$  we obtain  $J^{11} = 0.14eV$  (quite close to the band theory value). These parameters place the system well into the second order region of the phase diagram in apparent contradiction to experiments. In this case, the jump in specific heat is 19.24 (J/Mole) while the plasma frequency and magnetization are all continuous as a function of temperature, as shown in fig(7).

## V. CONCLUSION

We proposed a model to explain the combined metal/insulator, ferro/para magnetic phase transition of  $EuB_6$ . The splitting of the  $Eu$  derived conduction band due to the coupling to core electrons at each  $Eu$  site is found to be the origin of the phase transition. From the technical point of view, the new feature of our results is the detailed examination of the dynamical mean field free energy. The free energy calculation implies the transition is first order. By choosing the physically reasonable parameters, the available experimental data ( $T_c$ , jump in

plasma frequency, and jump in specific heat) are reasonably well reproduced if the picture is favored by band theory and transported is adopted. The calculated jump in specific heat is around two times greater than the experiments. We predict a metamagnetic phase transition at fields up to 8 tesla, if the temperature is within a few degrees of  $T_{c1}$ . We predict that the modest pressures will change the order of phase transition from first to second. The parameters found by photoemission lead to a second order transition, a disagreement with other experiments.

This work is supported by University of Maryland-Rutgers MRSEC.

- 
- [1] L. Degiorgi, E.Felder, H.R. Ott, J.L.Sarrao, and Z.Fisk Phys.Rev.Lett. **79**, 5134 (1997)
- [2] J.C.Cooley, M.C.Aronson, J.L.Sarrao, and Z.Fisk Phys.Rev.B **56** 14541 (1997)
- [3] S.Sullow, I.Prasad, M.C.Aronson, J.L.Sarrao, A.H.Lacerda, M.F.Hundley, A.Vigliante, and D.Gibs Phys.Rev.B **57** 5860 (1998)
- [4] S.Paschen, D.Pushin, M.Schlatter, P.Vonlanthen, H.R.Ott, D.P.Young, and Z.Fisk Phys.Rev.B **61** 4174 (2000)
- [5] S.Massidda, A.Continenza, T.M.Pascale, and R.Monnier, Z.Phys.B **102**, 83 (1997)
- [6] J. Kunes, and W.E.Pickett Phys.Rev.B **69** 165111 (2004)
- [7] J.D.Denlinger, J.A.Clack, J.W.Allen, G.-H.Gweon, D.M.Poirier, C.G.Olson, J.L.Sarrao, A.D.Bianchi, and Z.Fisk Phys.Rev.Lett. **89**, 157601-1 (2002)
- [8] M.C.Aronson, S.Sullow, Z.Fisk, M.Whitton, B.L.Brandt Phys.Rev.B **59** 4720 (1999)
- [9] A.Georges, G.Kotliar, W.Krauth, and M.Rozenberg, Rev of Modern Physics **68**, 13 (1996)
- [10] B.Michaelis, and A.J.Millis Phys.Rev.B **68** 115111 (2003)
- [11] We included a magnetic field coupling only to the core spin because we only want to express the free energy as a function of the core spin magnetization, not the total magnetization. In fact, if one wants to express the free energy as function of total magnetization, our answer should be a good approximation since the  $g$  factor is 1/2 for free electron while 7/2 for core spin.